Ultrasonics - Sonochemistry 56 (2019) 55–62

Contents lists available at ScienceDirect

Ultrasonics - Sonochemistry

journal homepage: www.elsevier.com/locate/ultson

Selective production of furfural from the dehydration of xylose using Zn doped CuO catalyst

Rahul Kumar Mishra, Vijay Bhooshan Kumar, Amudavalli Victor, Indra Neel Pulidindi, Aharon Gedanken*

Bar Ilan Institute for Nanotechnology and Advanced Materials, Department of Chemistry, Bar-Ilan University, Ramat-Gan 52900, Israel

ARTICLE INFO

Keywords:
Zn doped CuO NPs
Sonochemistry
Xylose dehydration
Furfural production

ABSTRACT

Furfural is a versatile biomass-derived platform compound used for the synthesis of several strategic chemicals. The sonochemically synthesized Zn doped CuO nanoparticles (NPs) were used for the production of furfural. The catalytic activity of the Zn doped CuO NPs was examined, as a model, during the dehydration reaction of xylose to furfural. In addition to that, we have also compared the catalytic activity of the Zn doped CuO NP with ZnO NPs, ZnO bulk, CuO NPs, CuO bulk, etc. This nanoscale catalyst (Zn doped CuO NP) has a large surface area, which enhances its catalytic activity and enables it to completely convert the xylose to furfural at 150 °C within 12 h without any trace of by-products, as confirmed by HPLC, ^{13}C NMR and ^{1}H NMR. HPLC analysis demonstrated that the yield of furfural is up to 86 mol %, compared to the 45 mol % obtained with ZnO NPs, ZnO bulk, CuO NPs, CuO bulk, etc. as catalysts.

1. Introduction

Furfural is a chemical of strategic importance that could be produced from hemicellulose rich biomass. Furfural serves as a potential precursor for the production of jet and diesel fuel range alkanes for transportation applications [1–3]. Apart from fuels production, furfural serves as a feedstock for the synthesis of several value added chemicals such as furfuryl alcohol, furan, liquid alkane's gasoline diesel, and hydroxy methyl furfural [4,5]. Furfural (2-furfuraldehyde) is currently obtained through the dehydration of pentoses, and an average of 250,000 tons-per year are produced in China, where over 70% of the global production is located [6]. The theoretical yield of furfural production from pentosan is 73% and current industrial processes operate with ~33% of the theoretical yields [7].

One of the most difficult struggles in the world today is its rapidly diminishing energy resources. The current research activities focus on using two main strategies: (a) the use of heterogeneous selective acid-catalysts and (b) the improvement of reaction systems [8]. The use of solid catalysts gathers most of the attention, especially since it shows the biggest potential of advancement beyond the current state-of-the-art, and especially due to their easy post-separation through a simple filtration step. The catalysts must feature surface acidity, product selectivity through textural property adjustment and enhanced hydrothermal stability [9]. The most studied solid acids are zeolites [10], which are highly structured crystalline microporous inorganic aluminosilicates containing channels with very well-defined pores of 0.5–1.3 nm [11,12]. Moreover, in the last decade, production of materials in the nano regime led to new innovations and improvements in science and industry. One of the advantages of materials in the nano scale is the enhancement of catalytic activity. Branca et al. reported on the acidic pyrolysis of corncobs for furfural production at 800 K in a packed-bed reactor using several catalysts (H_2SO_4, H_3PO_4, H_3BO_3, $(NH_4)_2SO_4$, $ZnCl_2$, $NiCl_2$, $MgCl_2$, and $Fe_2(SO_4)_3$). Metal oxide nanoparticles such as CuO, ZnO and MgO have biomass energy conversion capability [13,14].

Current commercial process of furfural production used sulphuric acid as the catalyst and high pressure steam provides the heat energy for the reaction. The yield of furfural is not greater than 45–50 wt% due to the formation of by products (humins) by the reaction between xylose and furfural [15]. The use of an heterogeneous catalyst with active sites of optimal acidity would improve the selectivity of the process resulting in higher yields of furfural [16,17]. Development of a sustainable, atom and energy efficient catalytic process for the conversion of biomass to furfural is the rate determining step towards a transition to non-fossil fuel based economy. The current commercial processes for furfural production employs concentrated mineral acids for the hydrolysis of hemicellulose to xylose and its subsequent dehydration to furfural. The use of such homogeneous acid catalysts has several

* Corresponding author.
E-mail address: gedanken@mail.biu.ac.il (A. Gedanken).

https://doi.org/10.1016/j.ultsonch.2019.03.015
Received 16 July 2018; Received in revised form 11 March 2019; Accepted 14 March 2019
Available online 15 March 2019
1350-4177/ © 2019 Elsevier B.V. All rights reserved.

Table 1
Catalytic pathways for the production of furfural.

Catalyst	Feedstock	Reaction conditions	Furfural yield (mol.%)	References
H_2SO_4, NaCl/$FeCl_3$ in water/toluene	Xylose	5 h, 170–185 °C,	83	[19]
SO_3H functionalized ionic-liquid under microwave irradiation	Xylose	1 h, 100 °C	85	[20]
EMIM/H_2SO_4 (1-ethyl-3-methylimidazolium hydrogen sulfate ([EMIM][HSO_4])) in water/toluene	Xylose	6 h, 180 °C	84	[21]
Water/Toluene; H-Faujasite Si/Al = 15	Xylose	6 h, 170 °C	90–95	[22]
Mixed solvents (water/dimethyl sulfoxide/tetrahydrofuran); Beta zeolite	Xylose	6 h, 200 °C	42	[23]
Water, dimethyl sulfoxide (DMSO) and a mixture of water and toluene (water/toluene) H-zeolites	Xylose	4 h, 140 °C	25	[24]
Water/toluene; layered zeolite Nu-6(1)	Xylose	4 h, 170 °C	47	[25]
Water/toluene; Zr–W–Al-mesoporous nanoparticles	Xylose	2 h, 170 °C	50	[26]
Water; ZrO_2–TiO_2	Xylose	5 mins, 300 °C	10	[27]
Water/toluene; TiO_2-graphene oxide	Xylose	10 mins, 170 °C	68	[28]
Water: β-Ga_2O_3	Xylose	12 h, 170 °C	94	[29]
Water: Zn doped CuO	Xylose	12 h, 150 °C	86	Current study

problems like formation of reaction by-products, corrosion to industrial installations, neutralization of the spent acid catalyst, reduced yield of desired product and waste management [16,17]. Use of selective and active heterogeneous catalyst would substantially reduce the production cost of furfural in addition to making the process environmentally friendly [18]. Towards solving the aforementioned issues, several researchers have attempted to develop a sustainable catalytic process for furfural production as summarized in Table 1.

In a previous work, a detailed study about new antibacterial nanoparticles of Zn doped CuO ($Cu_{0.89}Zn_{0.11}O$) was conducted [30,31]. Doping CuO with Zn ions leads to a significant increase of the antibacterial activity as compared to CuO or ZnO NPs [30,31]. Recently, $Cu_{0.89}Zn_{0.11}O$ was used for delaying the onset of catheter-associated urinary tract infections [32]. The current paper is probing the catalytic activity of a facile, efficient, surfactant free and acid-base free sonochemically synthesized Zn doped CuO NPs. The catalyst exhibits good activity and selectivity for the conversion of xylose to furfural. This solid catalyst can be easily separated from the product and reused for the conversion of biomass to important platform chemicals. Possible mechanism for the conversion of xylose to furfural is suggested. As a model for catalysis, furfural is a versatile biomass-derived platform compound for the synthesis of several strategic chemicals, which are currently derived from petroleum [33–36]. Xylose, obtained from the hydrolysis of hemicellulose, is an abundant and underutilized substrate. The conversion of pentose sugars to value-added products is still a pending key issue in biorefinery.

The current research focuses on two main strategies: a) the use of a heterogeneous as well as a selective $Cu_{0.89}Zn_{0.11}O$ catalyst and b) the improvement of the process of furfural production from xylose (Scheme 1) and its detailed possible mechanism.

2. Materials and methods

2.1. Chemicals

All the reagents were of chemical grade and used as received. Zinc oxide, ZnO (product no. Z-0875) in the bulk form was purchased from Sigma. Copper oxide, CuO (product no. 1317-38-0) in the bulk form was purchased from Aldrich Chem. Co. Zinc acetate dihydrate (product no. 383058) and copper acetate monohydrate (product no. 217557) were purchased from Sigma Aldrich.

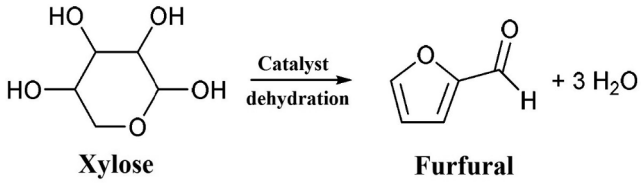

Scheme 1. Dehydration of xylose to furfural.

2.2. Synthesis of Zn doped CuO, CuO and ZnO nanoparticles

Typically, 3:1 M ratio of Cu:Zn was maintained for the wet synthesis of Zn-CuO nanoparticles. To maintain this molar ratio, 0.15 g of copper acetate monohydrate and 0.055 g of zinc acetate dihydrate were dissolved in 10 mL of double distilled water by stirring for 15 min. Specific volume ratio of 9/1 (ethanol/water) was maintained by adding 90 mL of ethanol in the fully solubilized 10 mL copper acetate monohydrate and zinc acetate dihydrate solution. This solution was then subjected to sonochemical irradiation with a high intensity ultrasonic Ti-horn (20 kHz, 750 W at 40% efficiency, Sonics & Materials VCX600 Sonofier). The ultrasonic intensity applied throughout the experiments is 45 W cm^{-2} unless stated otherwise. After 10 min of ultrasonic irradiation, a rise in temperature was observed which was noticed at 55 °C. To maintain a pH ~ 8, 0.8 mL of an aqueous solution of ammonium hydroxide (28–30%) was added in the reaction cell. A color change in the reaction mixture was observed after the addition of ammonium hydroxide solution, from pale blue to dark blue and then stabilized as dark brown color. The reaction mixture was chilled in an ice bath whereby the temperature was recorded as 30 °C. The sonochemical reaction process continued for 1 h. The resulting product was washed repeatedly with double-distilled water and ethanol to clean the impurities and traces of ammonia and then dried under vacuum overnight which yielded $Cu_{0.89}$ $Zn_{0.11}O$ [30,31]. To maintain the same amount of the precursor material, 0.2 g of copper acetate monohydrate was dissolved in 10 mL of double-distilled water. After this step, the synthesis of CuO and ZnO nanoparticles followed the same procedure as stated above.

The reactant (xylose, xylan, L-arabinose) if any (unreacted) as well as the reaction products (furfural, lactic acid, formic acid, levulinic acid and 1, 3 propane diol) were analyzed using C18 column. The mobile phase is a mixture of water and MeOH (10:90) for the analysis of furfural and 30:70 for the analysis of sugars. The concentrations of the reactants and products were deduced from the calibration plots prepared using standards. D-xylose conversion (C, mol. %) and furfural yield, (Y, mol. %) were calculated by the following Eqs. (1) and (2): [8]

$$D-Xylose\ conversion\ (C,\ mol\%) = \frac{[(Initial\ xylose\ amount,\ mol) - (Final\ xylose\ amount,\ mol)]}{[Initial\ xylose\ amount,\ mol]} \times 100 \quad (1)$$

$$Furfural\ yield,\ Y\ (mol\%) = \frac{[Final\ furfural\ amount,\ mol]}{Initial\ xylose\ amount,\ mol} \times 100 \quad (2)$$

3. Results and discussion

3.1. Characterization of Zn doped CuO

The characterization process of Zn doped CuO was carried out

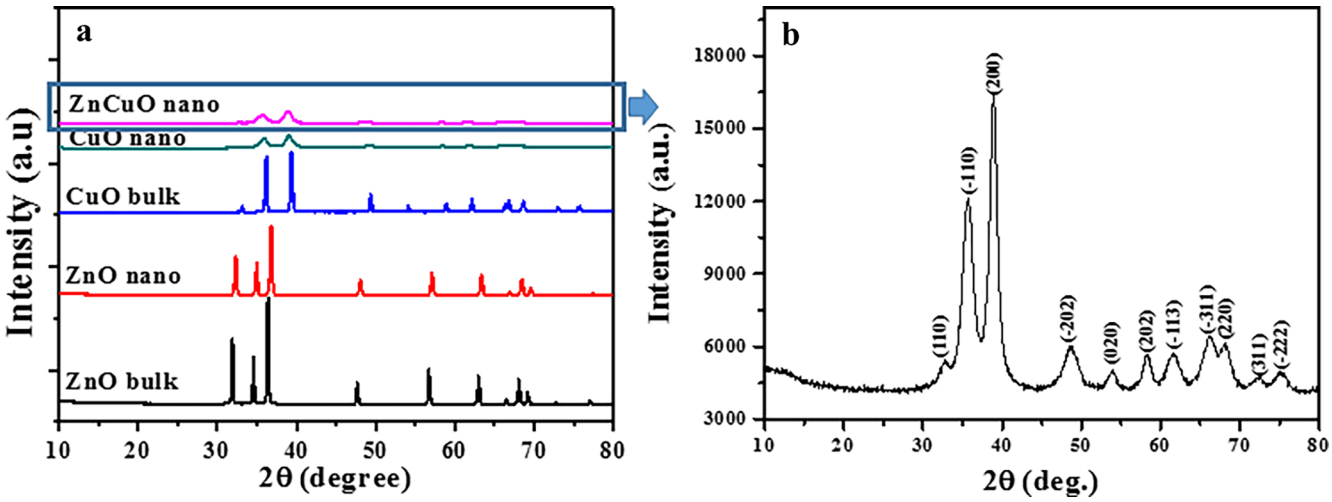

Fig. 1. XRD patterns of (a) ZnO (bulk), ZnO (nano), CuO (bulk), CuO (nano), Zn CuO nano, (b) ZnCuO nano plot, Intensity vs. 2theta.

identical to the description published elsewhere [30]. It included a variety of physicochemical techniques, like, XRD, SEM, and TEM to probe the properties of the catalyst: The obtained product was dried in vacuum overnight. The crystal structure of the Zn doped CuO NPs was confirmed by XRD analysis (Fig. 1). All the peaks in the XRD are assigned to monoclinic CuO. The peaks at 2θ = 32.51, 35.60, 38.70, 48.67, 53.91 58.32, 61.75, 66.22, 68.14 and 72.47 are assigned to the (1 1 0), (−1 1 0), (2 0 0), (−2 0 2), (2 0 2), (−1 1 3), (2 2 0), (3 1 1) and (−2 2 2) reflection lines of the monoclinic system. No peaks relating to ZnO or any other impurities were observed. However, the peaks of CuO were slightly shifted (Δ2θ = 0.2) towards higher angle and were broadened. The cell parameters of the CuO lattice (in Å) were changed from: a = 4.689; b = 3.420; c = 5.130 for CuO to a = 4.683; b = 3.420; c = 5.203 for the synthesized material. The changes in the lattice parameters confirm the doping of zinc into copper oxide lattice.

The morphology of sonochemically synthesized Zn doped CuO NPs was probed by high-resolution transmission electron microscopy (HRTEM). Fig. 2a and b reveal the homogeneous and uniform size of Zn doped CuO NPs with laminar shape. The calculation of the size-distribution of the doped particles was performed by Image J software based on measuring 100 Zn doped CuO NPs on the HRTEM image. The calculation yields a nearly normal distribution curve with a maximum size of around 6 nm. HRTEM images of Zn doped CuO NPs show that the NPs are highly crystalline, with a d-spacing of 0.26 nm. The d-spacing is in perfect correlation with X-ray diffraction (XRD) measurement (Fig. 1).

The surface morphology as well as the distribution of various elements in the Zn doped CuO catalyst were probed by SEM analysis and the corresponding images are shown in Fig. 2c–f. The presence as well as the uniform distribution of Zn throughout the CuO catalyst is observed.

Sonochemistry emerged as a novel approach for the synthesis of several types of nanomaterials. It is based on the use of high-intensity ultrasound (~20 kHz) to create acoustic cavitation in liquid media. Moreover, acoustic cavitation directly enhances the chemical reactions of Zinc acetate and Copper acetate, respectively. Ultrasound is directly employed in chemical reactions of Zinc acetate and Copper acetate in the water ethanol mixture, which can also be thermally driven. It is also being reported in literature that microbubbles can act as an adjuvant for the sonochemical reaction. Moreover, microbubbles can further enhance the thermal effects, which is crucial for the formation of $Cu_{0.89}Zn_{0.11}O$ NPs. It is also important to emphasize that sonochemistry, at least for metal oxide NPs, creates an unorganized and perturbed unit cell with many vacancies and dislocations. This features are desirable for the catalytic activity of the $Cu_{0.89}Zn_{0.11}O$ NPs.

3.2. Biomass conversion

3.2.1. Screening of catalysts for the selective production of furfural from xylose

A variety of metal oxides CuO (bulk and nano), ZnO (bulk and nano), Zn doped CuO (nano) were tested for the conversion of xylose to furfural in a hydrothermal reaction at 170 °C for 12 h with a catalyst to substrate ratio (wt/wt%) of 1:5. The reaction products after the reaction were analyzed by ^{1}H and ^{13}C NMR. The Zn doped CuO catalyst yielded selective formation of furfural from xylose. Moreover, almost complete conversion of xylose to furfural with minor amount of levulinic acid is achieved after the reaction. This is not the case with either pure CuO or ZnO, either in their bulk or nano forms. Thus, ZnCuO NPs are a selective catalyst for the dehydration of xylose to furfural. ^{1}H NMR spectra of the reaction products obtained using Zn doped CuO, CuO bulk, CuO nano, ZnO nano and ZnO bulk for the conversion of xylose were shown in Fig. 3. Irrespective of the catalyst used, all the products contained the desired product furfural as evident from the characteristic signals (6.7, 7.5, 7.9 and 9.4 ppm). In the case of Zn doped CuO catalyst, signals typical of furfural alone were observed Fig. 3(a) and also signals typical of xylose were absent (signals in the range of 3–4 ppm). On the contrary, in the case of other MO (metal oxide) catalysts, signals characteristic of other reaction products like levulinic acid and lactic acid were also observed as marked in Fig. 3.

Moreover, the substrate xylose is not completely converted under the reaction conditions. Thus, Zn doped CuO is screened out for further optimization of reaction parameters for the highest production yield of furfural from xylose. This result is further substantiated by the ^{13}C NMR analysis. The ^{13}C NMR spectra of the corresponding products are shown in Fig. S2 (see the Supporting information). In the case of the reaction product with Zn doped CuO as catalyst, signals typical of furfural (112.8 (C5), 121.5 (C4), 148.3 (C3), 153.1 (C2) and 177.9 (C1) ppm) alone were observed. Moreover, the signals characteristic of the reaction substrate, xylose (in the range of 60–100 ppm) were absent. On the contrary, in the case of other MO catalysts, the peaks typical of xylose were observed. So, either CuO (bulk and nano) or ZnO (bulk and nano) are not as active and selective as Zn doped CuO NPs. Further studies were carried out with the intention of understanding the selective

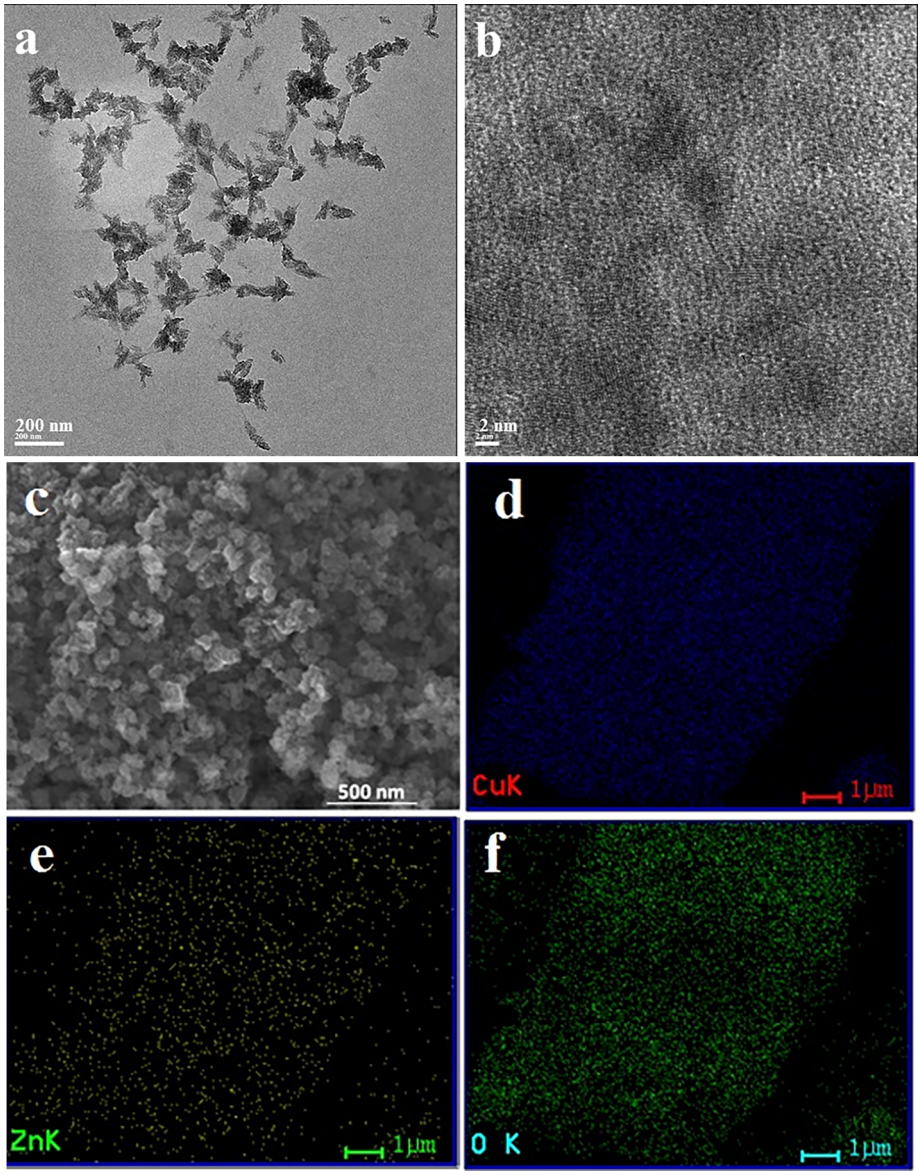

Fig. 2. (a) HRTEM images of Zn doped CuO, (b) magnified image of "a". (c) SEM image and elemental mapping of (d) Cu, (e) Zn, and (f) O in Zn doped CuO.

dehydrating ability of Zn doped CuO and to understand the possible reaction pathway and the active site for the catalytic transformation of xylose to furfural.

3.2.2. Effect of ratio of catalyst and reactant (wt/wt%) on xylose conversion and furfural yield

The use of smaller amounts of catalyst is preferred in an industrial process from economics point of view. The current study identifies the minimum amount of catalyst required for the complete and selective conversion of a given amount of xylose to furfural. At a catalyst to xylose weight ratio of 1–5, complete conversion of xylose exclusively to furfural is observed. When the amount of substrate is much higher (10 or 50 times) than that of the catalyst, even though the production of furfural is selective, xylose conversion is not complete. The ^{1}H and ^{13}C NMR spectra of the reaction products obtained under hydrothermal conversion of xylose to furfural are shown in Fig. 4 in support of the above deductions.

3.2.3. Optimization of reaction time for xylose conversion to furfural

The hydrothermal reaction time was optimized for the complete conversion of xylose to furfural. Shorter reaction times are often preferred in any chemical production process owing to the market demand of the product.

The minimum time required for the complete conversion of xylose to furfural using Zn doped CuO as catalyst is found to be 12 h. The hydrothermal conversion of xylose was carried out for different reaction times, namely, 2, 4, 8 and 12 h. The reaction is carried out at a hydrothermal reaction temperature of 150 °C and a substrate to catalyst ratio of 5: 1 (wt/wt). In each instance, the reaction product was analyzed by ^{1}H and ^{13}C NMR spectra of the products as a function of reaction time as shown in Fig. 5. Only in the case of the product obtained at 12 h reaction time, the signals typical of the substrate, xylose are absent indicating the complete conversion of xylose. In the case of products obtained at reaction times shorter than 12 h, the substrate is not completely converted. Irrespective of the reaction time, the product selectivity is exclusively towards furfural. For comparison, the NMR (^{1}H

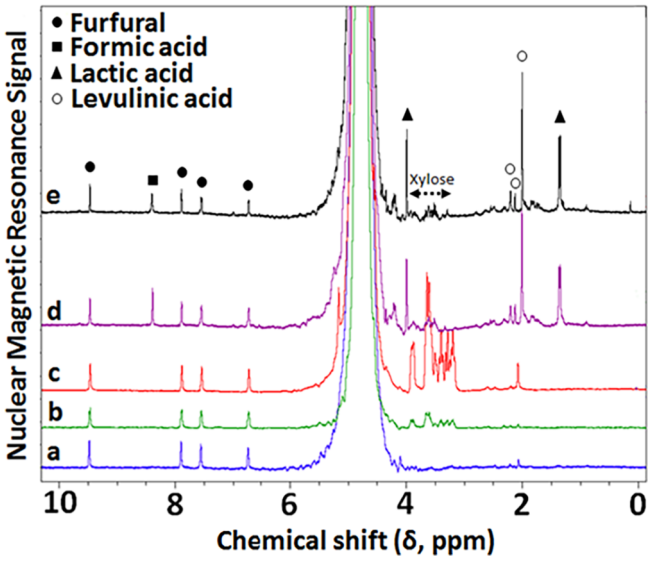

Fig. 3. ^{1}H NMR spectra of reaction products obtained using (a) Zn doped CuO, (b) CuO bulk, (c) CuO nano, (d) ZnO nano and (e) ZnO bulk (hydrothermal reaction conditions: 150 °C; 12 h; 5:1 wt% ratio of reactant and catalyst).

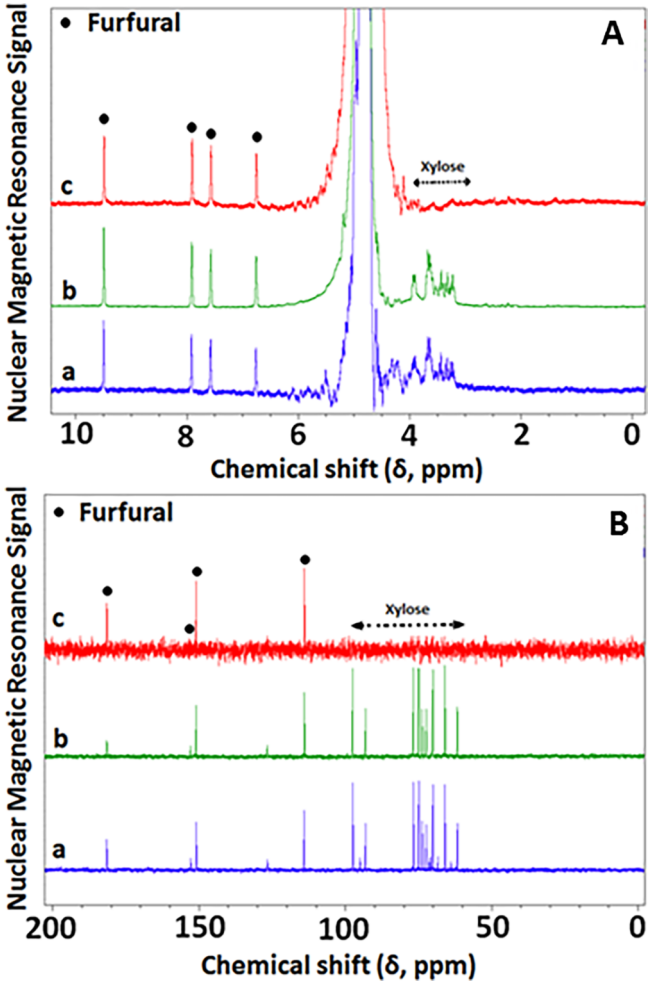

Fig. 4. ^{1}H (A) and ^{13}C NMR spectra (B) of reaction products obtained with different catalyst to reactant ratios (wt/wt%) (a) 1:50, (b) 1:10, (c) 1: 5; (Catalyst: Zn doped CuO; reactant: xylose; hydrothermal reaction conditions: 150 °C; 12 h).

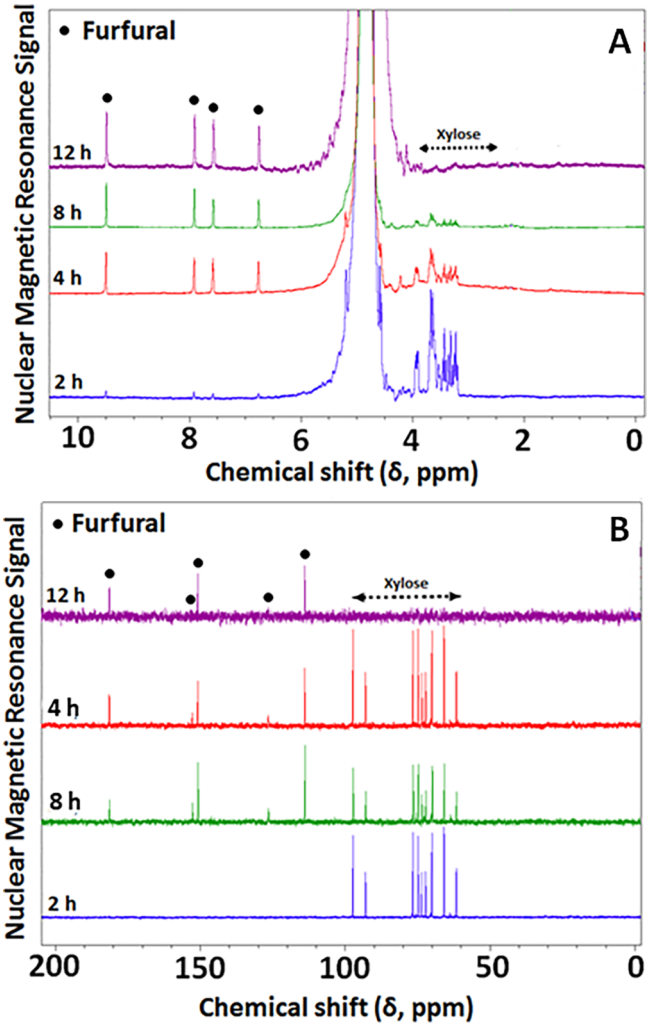

Fig. 5. ^{1}H (A) and ^{13}C NMR spectra (B) of reaction products obtained with different reaction times (2, 4, 8 and 12 h) (hydrothermal reaction conditions: 150 °C; Zn doped CuO: xylose = 1:5 (wt/wt%)).

and ^{13}C) spectra of authentic samples of xylose and furfural are shown in Fig. S3.

3.2.4. *Effect of the hydrothermal reaction temperature on xylose conversion to furfural*

The hydrothermal reaction for the conversion of xylose to furfural was carried out at different reaction temperatures, namely, 80, 150 and 180 °C. Having found in Section 3.2.3, that the optimal time for the complete conversion of xylose selectively to furfural, with Zn doped CuO catalyst, as 12 h, at 150 °C; the present experiment in Section 3.2.4, was aimed at knowing the course of xylose conversion at a temperature higher and lower than 150 °C. Since it is obvious that, a temperature lower than 150 °C (namely 80 °C) may require much longer time than 12 h for completion and a temperature higher than 150 °C (namely at 180 °C) requires shorter time than 12 h, the reactions at 80 and 180 °C were performed respectively for 48 and 4 h. Even after 48 h of reaction at 80 °C, xylose could not be dehydrated in the presence of Zn doped CuO catalyst. This is noticed from the presence of intense signals of xylose and also the absence of furfural in the reaction product [Fig. 6A (a) and B (a)].

The xylose conversion reaction was also studied at a temperature higher than 150 °C but for a duration of 4 h to check whether a

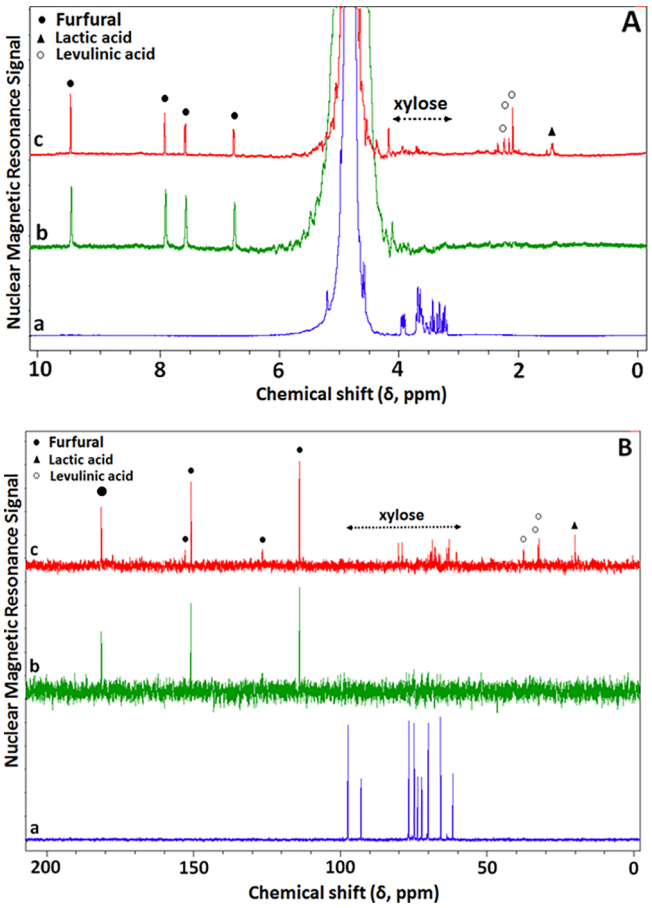

Fig. 6. Effect of hydrothermal reaction temperature ((a) 80 °C, 48 h (b) 150 °C, 12 h and (c) 180 °C, 4 h) on the conversion of xylose to furfural (Catalyst: Zn doped CuO; hydrothermal reaction conditions: 5:1 wt% ratio of reactant and catalyst); (A) ^{1}H and (B) ^{13}C NMR spectra.

complete conversion of xylose to furfural could be achieved in a shorter time. During these reaction conditions (180 °C, 4 h) with other conditions being the same, xylose conversion is not complete. Moreover, almost complete conversion of xylose is achieved after the reaction [Fig. 6A(c) and B(c)]. Trace amounts of levulinic and lactic acid were noticed as side products. For comparison, the ^{1}H and ^{13}C NMR of the reaction products obtained at a reaction temperature of 150 °C for 12 h are shown in Fig. 6A(b) and B(b), which show absence of xylose signals and also the exclusive formation of furfural from the dehydration of xylose.

Thus, the best hydrothermal reaction conditions for the selective dehydration of xylose to furfural using ZnCuO NPs as catalyst are: a catalyst to substrate ratio (wt/wt%) of 1:5; reaction temperature of 150 °C and a reaction time of 12 h.

3.3. Significance of doping of Zn in the CuO lattice structure for the selective production of furfural from xylose

So as to evaluate if the doping of Zn in the CuO lattice is crucial for the selectivity of $Cu_{0.89}Zn_{0.11}O$ catalyst, a physical mixture of CuO (88 wt%) and ZnO (12 wt%) nanoparticles mimicking the stoichiometric amounts of Cu and Zn in the dopant ($Cu_{0.89}Zn_{0.11}O$) is prepared and used as a catalyst for the conversion of xylose. Typical reaction comprises of taking in a hydrothermal reactor 0.5 g of xylose in 20 mL DDW and adding 0.1 g of physical mixture of CuO (0.088 g) and ZnO (0.012 g). The contents were then subjected to hydrothermal reaction

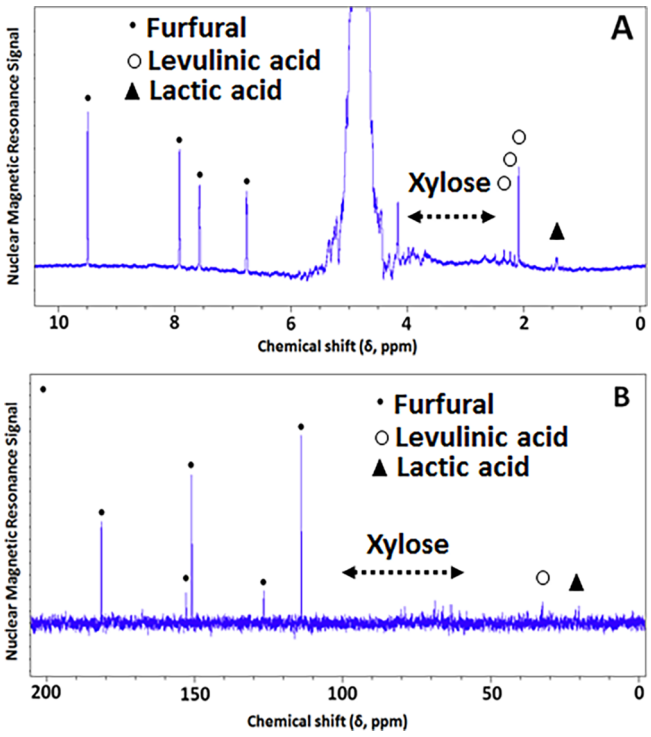

Fig. 7. Evaluation of catalytic activity of physical mixture of CuO and ZnO (1:1 wt%).

under optimal reaction conditions (150 °C, 12 h). Even though the major reaction product of the dehydration of xylose is furfural, other reaction byproducts like levulinic and lactic acid were observed. Moreover, traces of unreacted xylose were also observed as evident from the NMR analysis (Fig. 7A and B). This proves that the selective conversion of xylose to furfural in the case of Zn doped CuO could be attributed to the doping of Zn in the CuO lattice and similar activity and selectivity could not be achieved by mere physical mixing of the respective oxides.

3.4. Reaction mechanism for the conversion of xylose to furfural Zn doped CuO catalyst

Malka et al. has prepared the $Cu_{0.89}Zn_{0.11}O$ NPs, and demonstrated its strong biocidal effect, about thousand times stronger than both the pristine ZnO or CuO NPs. Later, Malka et al. has attributed this unique property to the perturbed structure of the $Cu_{0.89}Zn_{0.11}O$ as well as ZnO and CuO prepared sonochemically. The sonochemically prepared metal oxides have plenty of dislocations, vacancies as compared with the same size particles purchased from a commercial company. Further insights into the role of doping of Zn into CuO lattice on the mechanism of dehydration of xylose to furfural are provided in Scheme 2.

Generally, metal oxides consist of a metal and oxygen ionic bond. The coordination of metal and oxygen ions is incomplete compared to their bulk form. Thus, the metal cations and oxide anions are partially uncoordinated exposed on the metal oxides crystal surface which can act as acids and bases, respectively. Hence, coordinatively unsaturated cations result into active Lewis acid sites. The coordinatively unsaturated cations are exposed on the surface of ionic oxides can interact with basic compounds by forming a new coordination bond. The overall coordination is either completed or increased by the formation of new coordination on the surface of metal cations [37]. In this mechanism of the production of furfural from xylose, Zn and Cu act as Lewis acid sites and catalyze the reaction in the forward direction via xylose

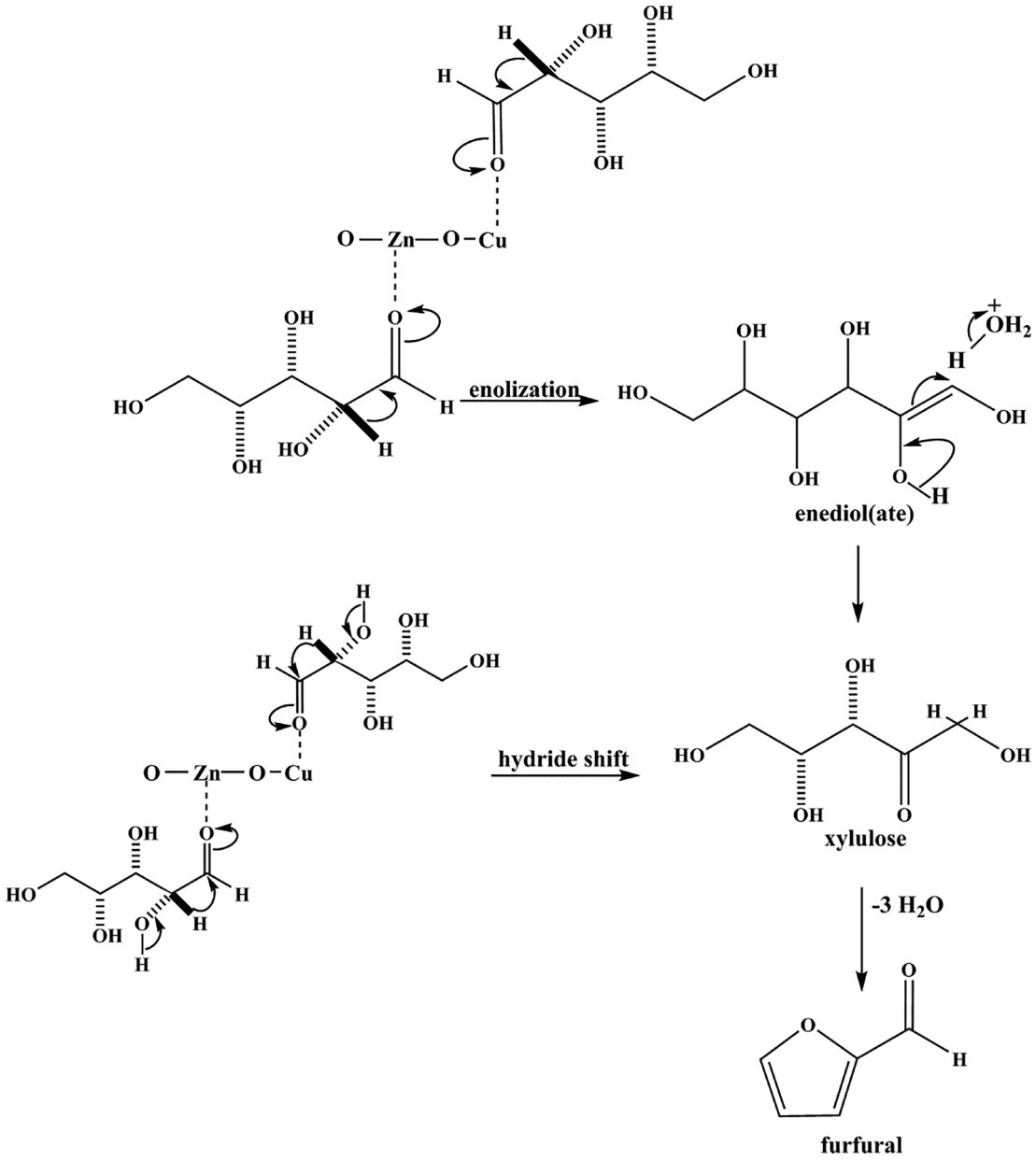

Scheme 2. Possible reaction mechanism for the dehydration of xylose to furfural on Zn doped CuO.

isomerization with a 1,2-hydride shift. Then, xylulose is converted into an oxicarbenium ion by Lewis acids, Zn and Cu. The subsequent deprotonation of these species produces an enol and further yields furfural by losing three molecules of water [38]. In the proposed mechanism, the yield of furfural from the Zn doped CuO NPs is higher and more selective than the corresponding ZnO and CuO (both bulk and NPs). This is due to the highly defective structure of the Zn doped CuO NPs which resulted due to the incorporation of Zn into CuO lattice [39]. The highly defective structure of Zn doped CuO NPs provide more active sites for xylose to react and the characters of both the ZnO and CuO are present. The higher and selective yield of furfural from xylose catalyzed by Zn doped CuO NPs also points out to its increased Lewis acidity. For comparison, the reaction mechanism involved in the conversion of xylose to furfural using CuO and ZnO catalysts is shown in Figs. S4 and S5 respectively.

3.5. Quantification of furfural produced from xylose under best hydrothermal reaction conditions by HPLC

The quantification of the furfural product was performed using HPLC analysis. As shown in Fig. 8, Zn doped CuO is more active and selective catalyst for the dehydration of xylose to furfural than either CuO or ZnO. The superiority of Zn doped CuO is also reflected in the absence of any appreciable amount of by-products, and the yield of furfural approaches 62 wt%. The selectivity towards the production of furfural reaches 89% for Zn doped CuO while for other catalysts (ZnO, CuO, etc) the value is less than 50%.

4. Conclusion

A novel surfactant free, solid acid Zn doped CuO catalyst was used for the first time for the biomass conversion using hydrothermal

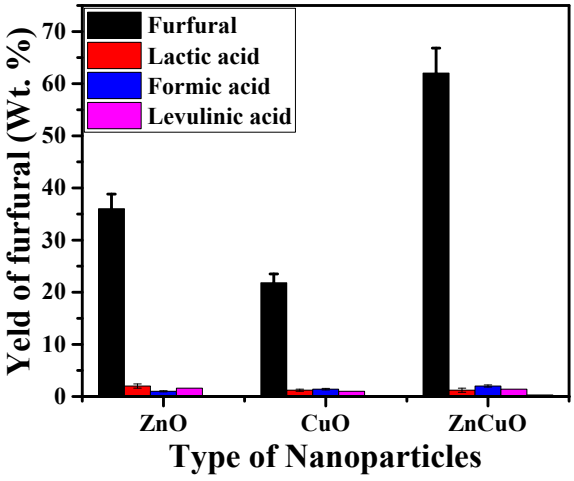

Fig. 8. Yield of furfural as a function of catalyst used for the dehydration of xylose.

reaction. The Zn doped CuO catalyst exhibits better activity and selectivity for the conversion of xylose to furfural compared to ZnO, and CuO. The detailed mechanism for the conversion of D-xylose to furfural is proposed. The current findings may be utilized for different biomass repositioning to selectively obtain industrially important compounds. The present concept possesses distinct potential in the present time of energy crisis owing to its higher selectivity and no mass loss in the catalyst for furfural production.

Acknowledgements

The authors acknowledge with thankfulness the generous support of the Israel Science Foundation (ISF, Grant No. 598/12) and the Israel Ministry of Science, Technology and Space (Grant Nos. 3-9802 and 3-99763) by funding this work.

Appendix A. Supplementary data

Supplementary data to this article can be found online at https://doi.org/10.1016/j.ultsonch.2019.03.015.

References

[1] J. Xu, N. Li, X. Yang, G. Li, A. Wang, Y. Cong, X. Wang, T. Zhang, ACS Catal. (2017) 5880–5886.
[2] A.D. Sutton, F.D. Waldie, R. Wu, M. Schlaf, L.A.P. Silks, J.C. Gordon, Nat. Chem. 5 (2013) 428–432.
[3] M. Balakrishnan, E.R. Sacia, S. Sreekumar, A.A. Gokhale, C.D. Scown, F.D. Toste, M. Balakrishnan, E.R. Sacia, S. Sreekumar, G. Gunbas, A.A. Gokhale, Proc. Natl. Acad. Sci. 112 (2015) E3969.
[4] J. Yang, S. Li, N. Li, W. Wang, A. Wang, T. Zhang, Y. Cong, X. Wang, G.W. Huber, Ind. Eng. Chem. Res. 54 (2015) (1837) 11825–11831.
[5] C. Grant, D. Deszcz, Y.-C. Wei, R.J. Martínez-Torres, P. Morris, T. Folliard, R. Sreenivasan, J. Ward, P. Dalby, J.M. Woodley, F. Baganz, Sci. Rep. 4 (2015) 5844.
[6] X. Tong, Y. Ma, Y. Li, Appl. Catal. A Gen. 385 (2010) 1–13.
[7] R. Xing, W. Qi, G.W. Huber, Energy Environ. Sci. 4 (2011) 2193.
[8] S. Le Guenic, F. Delbecq, C. Ceballos, C. Len, J. Mol. Catal. A: Chem. 410 (2015) 1–7.
[9] I. Agirrezabal-Telleria, I. Gandarias, P.L. Arias, Catal. Today 234 (2014) 42–58.
[10] P. Brazdausks, M. Puke, N. Vedernikovs, I. Kruma, Balt. For., 20 (2014) 106–114.
[11] J. Patarin, Angew. Chemie – Int. Ed. 43 (2004) 3878–3880.
[12] K. Tanabe, Appl. Catal. A Gen. 181 (1999) 399–434.
[13] N. Kumar, B. Stephanidis, R. Zenobi, A.J. Wain, D. Roy, Nanoscale 7 (2015) 7133–7137.
[14] H. Lee, J.A. Hong, Nanoscale Res. Lett. 12 (2017) 426.
[15] A. Corma Canos, S. Iborra, A. Velty, Chem. Rev. 107 (2007) 2411–2502.
[16] T. Ennaert, J. Van Aelst, J. Dijkmans, R. De Clercq, W. Schutyser, M. Dusselier, D. Verboekend, B.F. Sels, Chem. Soc. Rev. 45 (2016) 584–611.
[17] X. Li, P. Jia, T. Wang, ACS Catal. 6 (2016) 7621–7640.
[18] J. Bennett, K. Wilson, A.F. Lee, J. Mater. Chem. A 4 (2016) 3617–3637.
[19] C. Rong, X. Ding, Y. Zhu, Y. Li, L. Wang, Y. Qu, X. Ma, Z. Wang, Carbohydr. Res. 350 (2012) 77–80.
[20] J.C. Serrano-Ruiz, J.M. Campelo, M. Francavilla, A.A. Romero, R. Luque, C. Menéndez-Vázquez, A.B. García, E.J. García-Suárez, Catal. Sci. Technol. 2 (2012) 1828.
[21] S. Lima, P. Neves, M.M. Antunes, M. Pillinger, N. Ignatyev, A.A. Valente, Appl. Catal. A Gen. 363 (2009) 93–99.
[22] C. Moreau, R. Durand, D. Peyron, J. Duhamet, P. Rivalier, Ind. Crops Prod. 7 (1998) 95–99.
[23] R. Otomo, T. Tatsumi, T. Yokoi, Catal. Sci. Technol. 5 (2015) 4001–4007.
[24] S.B. Kim, S.J. You, Y.T. Kim, S. Lee, H. Lee, K. Park, E.D. Park, Korean J. Chem. Eng. 28 (2011) 710–716.
[25] S. Lima, M. Pillinger, A.A. Valente, Catal. Commun. 9 (2008) 2144–2148.
[26] M.M. Antunes, S. Lima, A. Fernandes, J. Candeias, M. Pillinger, S.M. Rocha, M.F. Ribeiro, A.A. Valente, Catal. Today 195 (2012) 127–135.
[27] A. Chareonlimkun, V. Champreda, A. Shotipruk, N. Laosiripojana, Bioresour. Technol. 101 (2010) 4179–4186.
[28] P.A. Russo, S. Lima, V. Rebuttini, M. Pillinger, M.-G. Willinger, N. Pinna, A.A. Valente, RSC Adv. 3 (2013) 2595.
[29] V.B. Kumar, R.K. Mishra, I.N. Pulidindi, Z. Porat, J.H.T. Luong, A. Gedanken, Energy Fuels 30 (2016) 7419–7427.
[30] E. Malka, I. Perelshtein, A. Lipovsky, Y. Shalom, L. Naparstek, N. Perkas, T. Patick, R. Lubart, Y. Nitzan, E. Banin, A. Gedanken, Small 9 (2013) 4069–4076.
[31] R.K. Mishra, Y. Shalom, V.B. Kumar, J.H.T. Luong, A. Gedanken, E. Banin, J. Mater. Chem. B 4 (2016) 6706–6715.
[32] Y. Shalom, I. Perelshtein, N. Perkas, A. Gedanken, E. Banin, Nano Res. 10 (2017) 520–533.
[33] C. Chang, X. Ma, P. Cen, Chinese J. Chem. Eng. 14 (2006) 708–712.
[34] X. Li, Y. Jiang, L. Wang, L. Meng, W. Wang, X. Mu, RSC Adv. 2 (2012) 6921.
[35] I.N. Pulidindi, B.B. Kimchi, A. Gedanken, Renew. Energy 71 (2014) 77–80.
[36] L. Peng, L. Lin, J. Zhang, J. Zhuang, B. Zhang, Y. Gong, Molecules 15 (2010) 5258–5272.
[37] L. Saad, M. Riad, J. Serb. Chem. Soc. 73 (2008) 997–1009.
[38] J.B. Binder, J.J. Blank, A.V. Cefali, R.T. Raines, Chem. Sus. Chem. 3 (2010) 1268–1272.
[39] J. Iqbal, T. Jan, S. Ul-Hassan, I. Ahmed, Q. Mansoor, U. Ali, F. Abbas, Md. Ismail, Facil synthesis of Zn doped CuO hierarchical nanostructures: structure, optical and antibacterial properties, AIP Adv. 5 (2015) 127112.